PERGAMON

Control Engineering Practice 7 (1999) 459–468

Active sonar-based bottom-following for unmanned underwater vehicles

M. Caccia*, G. Bruzzone, G. Veruggio

Consiglio Nazionale delle Ricerche, Istituto Automazione Navale, Via De Marini, 6, 16149 Genova, Italy

Received 5 December 1997; accepted 11 August 1998

Abstract

The problem of high-precision bottom-following in the proximity of the seabed for open-frame unmanned underwater vehicles (UUVs) is addressed in this paper. The suggested approach consists of the integration of a guidance and control system with an active multi-hypothesis extended Kalman filter, able to estimate the motion of the vehicle with respect to the bottom profile. The guidance module is based on the definition of a suitable Lyapunov function associated with the bottom-following task, while the motion controller is a conventional autopilot, performing autoheading, autodepth, and autospeed. The motion of the vehicle is estimated from range and bearing measurements supplied by a high-frequency pencil-beam profiling sonar. Moreover, a general-purpose sensor-based guidance and control system for advanced UUVs, able to manage active sensing-based guidance and motion estimation modules, is presented. An application of the proposed architecture to execute high-precision bottom-following using Romeo, a prototype UUV, developed by the Robotics Dept. of the Istituto Automazione Navale, is described. Experimental results of tests, conducted in a high-diving pool with the vehicle equipped with a sonar profiler, are presented.

Keywords: Underwater vehicles; Range sensing; Motion estimation; Extended Kalman filters; Guidance systems; Active sensing

1. Introduction

High-precision motion control of unmanned underwater vehicles (UUVs) at low speeds in the proximity of the seabed is required in many operational applications such as visual surveys of the seabed, mosaicking, censuses of marine life or features, and constant-speed dragging of sensors/samplers to obtain regular measurements. The operating vehicle, generally an open-frame UUV equipped with a scientific payload, is required to be able to follow the sea bottom at short distances (less than 2 m) at a speed of some tenths of centimeters per second (typically lower than 0.5 m/s).

The task of bottom-following, i.e., "maintaining a fixed altitude above an arbitrary surface whose characteristics may or may not be known" (Bennett et al., 1995), has been extensively treated in the literature in the case of torpedo-like, survey-class autonomous underwater vehicles (AUVs). In particular, the case of AUVs equipped with one or two downward-looking sonar altimeters, which measure the vehicle's distance from the bottom and enable it to estimate the seabed profile, has been investigated in Bennett et al. (1995). Aspects concerning the estimation of the bottom slope in relation to the vehicle, the management of transitions between different slope sections, and the relations between bottom-following and other tasks, are examined in Santos et al. (1995a, b).

In this paper the problem of bottom-following is addressed for a class of open-frame UUVs, moving at low speeds very close to the seabed. In these operational conditions, the use of high-frequency pencil-beam profiling sonars (which have a shorter operating range and ensure higher precision than traditional echo-sounders) and recursive filtering techniques allows high-precision estimates of the UUV motion with respect to the seabed profile. Recent experimental results have also demonstrated that estimator performances can be enhanced by feature-related control of the motion of the profiler sonar (Caccia et al., 1997).

*Corresponding author. Tel.: +39 010 6475612; fax: +39 010 6475600; e-mail: max@ian.ge.cnr.it.

0967-0661/99/$ - see front matter
PII: S0967-0661(98)00168-3

A general-purpose sensor-based guidance and control system for advanced UUVs, able to manage the active sensing-based guidance and estimation techniques mentioned above, has been designed. The architecture consists of conventional UUV autopilot and navigation systems, integrated with motion-task-oriented guidance, an environment-based motion estimator and external sensor controller modules, as discussed in Section 2, where the distinction between a task-independent lower level (autopilot and external sensor controller) and a task-based upper level, consisting of guidance and active estimation modules, is emphasized.

The bottom-following task is defined in Section 3. A guidance algorithm, based on the definition of a Lyapunov function of the error in the distance from the seabed and the choice of autopilot set-points to make it negative definite, is presented.

The bottom-estimation technique is discussed in Section 4. The bottom profile and its distance from the vehicle are estimated by an active multi-hypothesis extended Kalman filter, which processes the profiler sonar range and bearing measurements.

The proposed sensor-based guidance and control system has been implemented on Romeo, a prototype UUV developed by C.N.R.-I.A.N. for marine science applications and robotics research (Veruggio et al., 1996), and tested in a pool.

Section 5 describes the hardware and software architecture of Romeo, while experimental tests and results are presented in Section 6.

2. Sensor-based guidance and control system

A general-purpose sensor-based guidance and control system for UUVs is described below. Attention is focused on the guidance of the vehicle in respect to its operational environment. In this way, "external sensors", which measure interactions between the robot and the environment in preferred directions (Samson et al., 1991), are considered. Here the aspects of this architecture concerned with the execution of the task of bottom-following are presented, while an application to the horizontal motion guidance and control of a prototype UUV is described in Caccia et al. (1998). Since the unpredictability of subsea environments and the limitations of the state-of-the-art machine-intelligence techniques makes real-world operations reliable only in the presence of possible human intervention (Sayers et al., 1996), a basic requirement in developing guidance and control systems for operational UUVs is to enable the human operator to tele-operate the robot, by interacting with each level of the control architecture (Sheridan, 1989). In this way, a modular guidance and control system has been designed, integrating conventional autopilot and navigation modules with an "external sensors" controller, an active estimator of the motion in respect to the operational environment, and guidance modules. The resulting system architecture is depicted in Fig. 1, where submodules and data flow required to execute the bottom-following task are pointed out.

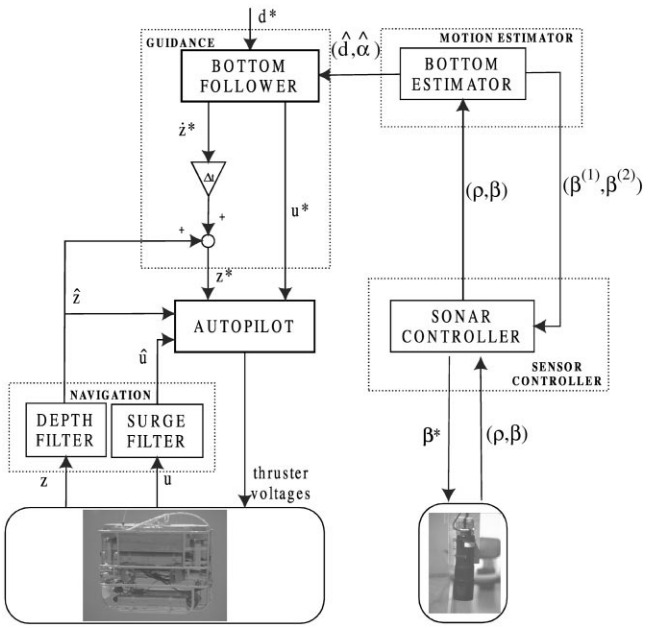

Fig. 1. Bottom-following architecture for UUVs.

The UUV *autopilot* controls the vehicle's heading, attitude (pitch and roll), depth, and horizontal speed (surge and sway). As discussed in Fossen (1994), in most practical applications, autopilots constituted by simple uncoupled controllers of PID-type are sufficient. In particular, typical survey applications can be executed by vehicles performing automatic control of heading (PID-type), depth (PID-type) and surge (PI-type). The autopilot is organized in four layers. The first layer is the automatic control mode, which generates the forces and torques to be applied to the vehicle to obtain the desired behavior. In the second layer, the thrust mapping function maps the required forces and torque in the vector of thrust to be applied to the actuators, according to the vehicle's thruster configuration and user-defined requirements such as low-power consumption or motion precision. In the third layer the voltage mapping function maps the thrust vector containing the desired motor thrusts into a voltage vector to be sent to the boards of the servo-motor drivers. Finally, in the lowest mode, each thruster voltage can be set directly.

The vehicle motion is estimated by the *navigation system*. Data supplied by a compass, a gyro, inclinometers, a depth-meter, a current-meter and/or a Doppler velocimeter, are integrated to estimate the vehicle kinematics state required by the Autopilot. In addition, the integration of acoustic positioning systems and/or linear

accelerometer measurements can allow the vehicle's absolute position to be estimated.

The autopilot and navigation systems are independent of the task the robot has to accomplish and are sufficient to enable the human pilot, helped by video feedback from a TV camera mounted on the vehicle, to tele-operate the vehicle. This is the case in many operational ROVs.

The *guidance system* generates autopilot set-points to perform motion tasks of different types. Since in the operational area, the vehicle moves in the proximity of environmental features such as the seabed or man-made structures, a number of operational motion tasks can be defined in respect to the interactions between the vehicle and its surroundings. These motion functions can be classified into safety tasks such as obstacle, bottom and surface avoidance, and environment-based tasks as bottom-following, ice-canopy following, and wall-following with a pre-defined orientation. Moreover, the vehicle can be required to move in an earth-fixed reference frame to operate in a well-defined area. In this case, free-space motion tasks are executed, such as reaching a target frame (position and orientation) and remaining stationary on site, even in the presence of disturbances (Caccia et al., 1998).

Underwater optic and acoustic visual sensors can provide feedback on the interactions between the UUV and the operational environment. Since it is possible to focus the attention of profiling sonars and pan-tilt TV-cameras in particular directions, the most advanced UUVs provide an *external sensor controller*, able to acquire data and to control the motion of these devices both in the environment and in the vehicle fixed reference frame.

In particular, high-frequency pencil-beam profiler sonars can provide high-precision measurements of the interactions between the vehicle and the environment at short ranges. In this case, the *sonar controller* pilots the profiler sonar head motion in order to satisfy the human operator and/or the requirements of the data-processing algorithm. The sonar profiler motion and data acquisition can be controlled at various levels. Continuous pings in a fixed direction, and clockwise and counterclockwise radar-like circular scans and sweeps in a circular sector are described in a vehicle/sensor-fixed reference frame. Sweeps between the absolute horizontal or vertical directions have to be described in an earth-fixed reference frame, and need vehicle heading or pitch data to be acquired. These different profiler motion modes correspond to different layers of the Sonar Controller.

The motion of the vehicle in respect to basic features detected in the operational environment is estimated by the *environment-based motion estimator*. Where it is possible to control the sensor attention, the estimator performances are increased by adopting task-driven and feature-related active sensing techniques. Task-driven control of visual attention can be performed independently of the estimation processing (Swayn and Stricker, 1993). For instance, when the task of obstacle detection is performed, a profiling sonar looks ahead, sweeping across a sector in the vehicle fixed reference frame. Feature-related control of visual attention allows the estimator performance to be improved, controlling the sensor movements on the basis of the result of the estimation processing. In the case of bottom-following, a more precise tracking of the desired distance from the seabed in the presence of sudden changes in the bottom profile is allowed by the availability of a high-precision estimator of the bottom slope and the vehicle's distance from the seabed. A feature-related control of the profiler sonar is performed to increase the precision in the slope estimate tracking the linear surface, which currently approximates the seabed profile. In particular, the bottom profile is tracked by the profiler sonar, sweeping a circular sector with extremes $\beta^{(1)}$ and $\beta^{(2)}$ (see Fig. 1), determined by the bottom estimator.

A more detailed description of the bottom-following and bottom-estimation modules is given in the next two sections.

3. Bottom-following: task definition and guidance module

Here, the task of bottom-following is defined as navigating at a fixed distance from the seabed, represented as an arbitrary surface whose characteristics may or may not be known. The interactions between the UUV and the seabed are measured by range data supplied by a high-frequency pencil-beam profiling sonar, sweeping the bottom profile along the vehicle's longitudinal direction. Fig. 2 depicts a UUV moving in the proximity of the

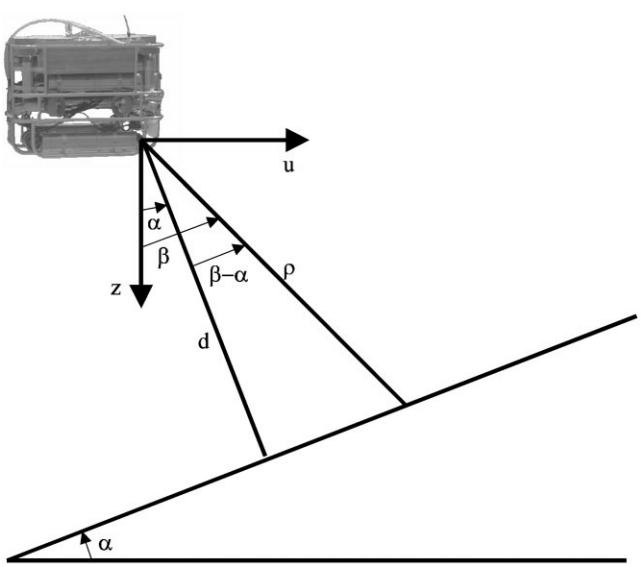

Fig. 2. Nomenclature for a bottom-following UUV.

seabed. Define z and u as the vehicle depth and surge, respectively, d as the distance of the vehicle from the bottom, α as the bottom slope, and ρ and β as the sonar range and bearing, respectively.

Since this research is focused on high-precision bottom-following for operational open-frame UUVs, which are generally structurally stable in pitch and roll, the vehicle pitch in not considered.

Referring to Fig. 2, the guidance task of bottom-following can be described by the function

$$e = d - d^*, \tag{1}$$

where d^* is the desired vehicle distance from the seabed.

It is possible to write the following Lyapunov function of the task variable e, which represents the distance error:

$$V = \tfrac{1}{2}e^2 = \tfrac{1}{2}(d - d^*)^2. \tag{2}$$

Since the speed of the vehicle in the direction perpendicular to the bottom profile is (see Fig. 2)

$$\dot{d} = -\dot{z}\cos\alpha - u\sin\alpha, \quad \alpha \in \left(-\frac{\pi}{2}, \frac{\pi}{2}\right), \tag{3}$$

the first time derivative of V can be expressed as

$$\dot{V} = -(d - d^*)(\dot{z}\cos\alpha + u\sin\alpha), \quad u > 0, \tag{4}$$

where the vehicle is assumed to move forward, i.e. $u > 0$.

$\dot{V}$ is negative definite if

$$\dot{z}\cos\alpha + u\sin\alpha = k(d - d^*), \quad k > 0,\ u > 0, \tag{5}$$

where k is a given constant.

Eq. (5) is satisfied by choosing

$$\begin{aligned} u^* &= \bar{v}\cos\alpha \\ \dot{z}^* &= -\bar{v}\sin\alpha + k\,\frac{d - d^*}{\cos\alpha}, \quad \bar{v} > 0, \end{aligned} \tag{6}$$

where $\bar{v}$ is the fixed vehicle speed in the direction parallel to the bottom profile, and the term $k(d - d^*)/\cos\alpha$ compensates for the bottom distance error. Of course, in real applications this component is saturated, obtaining

$$\begin{aligned} u^* &= \bar{v}\cos\alpha, \\ \dot{z}^* &= -\bar{v}\sin\alpha + \mathrm{sat}_w\left(k\,\frac{d - d^*}{\cos\alpha}\right), \end{aligned} \tag{7}$$

where sat_w stands for the saturation function, i.e.,

$$\mathrm{sat}_w(x) = \begin{cases} -w & \text{if } x < -w, \\ x & \text{if } |x| \leqslant w, \\ w & \text{if } x > w. \end{cases} \tag{8}$$

Since $V \geqslant 0$ and $\dot{V} \leqslant 0$, for the Barbalat lemma $\lim_{t\to\infty} V(t) = 0$, which complete the proof of convergence.

The reference heave value computed in Eq. (7) is transformed into the desired depth for the UUV autopilot on the basis of the estimated vehicle depth according to the following relation:

$$z^* = \hat{z} + \dot{z}^*\,\Delta t, \tag{9}$$

where z^* and $\hat{z}$ are, respectively, the reference and estimated depth, and Δt is the sampling time.

4. Bottom estimation

Referring to Fig. 2, the bottom estimator state and measurement equations are

$$\begin{aligned} d(k+1) &= d(k) + \dot{d}(k)\Delta t, \\ \dot{d}(k+1) &= \dot{d}(k) + w_{\dot{d}}(k), \\ \alpha(k+1) &= \alpha(k) + w_\alpha(k), \end{aligned} \tag{10}$$

$$\rho(k) = \frac{d(k)}{\cos[\beta_k - \alpha(k)]} + v(k) \tag{11}$$

which represent a linear system with a nonlinear and time-varying measurement channel affected by noise. The noise v is supposed to be Gaussian at zero mean and covariance R. The measurement equation is a function of the profiler bearing β_k which can be actively controlled by the motion-estimation module. The system noise $w_{\dot{d}}$ takes account of the slow changes in the vehicle depth, whose measurement is not considered by this filter.

The state of system (10) can be estimated by an extended Kalman filter, in consideration of the good results obtained in Cristi et al. (1996) and Caccia et al. (1997). The state noise w_α allows the filter to follow gradual changes in the bottom slope. However, particularly big values of w_α make the estimate more sensitive to measurement noise, so the resulting filter is unable to follow sudden slope changes without prejudicing high-precision estimation.

This problem can be tackled successfully by applying an active multi-hypothesis approach.

This approach basically consists of three actions:

1. track the current surface which approximates the bottom profile;
2. detect a change in the bottom slope;
3. estimate the new slope and go back to action 1.

In nominal conditions, the active estimator controls the profiler bearing on the basis of the current estimate of the bottom slope and of the memorized last tracked surface. The profiling sonar sweeps a sector centered orthogonally to the tracked reflecting surface:

$$\beta^{(1)} = \hat{\alpha} - \Delta\beta, \qquad \beta^{(2)} = \hat{\alpha} + \Delta\beta, \tag{12}$$

where $\beta^{(1)}$ and $\beta^{(2)}$ are the swept sector extremes, $\Delta\beta$ the swept sector semi-amplitude, and $\hat{\alpha}$ the estimated bottom slope. In addition, the active estimator memorizes the

last tracked surface slope. The profiler is forced to move forward every time the last tracked surface is detected. This feature-related control of the profiling sonar to track the current estimated surface allows the effects of the linearization of the measurement equation to be reduced, to avoid the alternate tracking of different surfaces and to minimize the presence of many missed sonar echoes when the vehicle follows a descending profile (Caccia et al., 1997).

The problem of detecting any change in the bottom profile and estimating the new slope of the bottom surface is successfully faced by means of a normalized square innovation test and a multi-hypothesis approach.

Calling $[\hat{d}\ \dot{\hat{d}}\ \hat{\alpha}]$ the estimated state, the innovation and its covariance are defined as

$$\varepsilon(k/k-1) = \rho(k) - \frac{\hat{d}(k/k-1)}{\cos[\beta_k - \hat{\alpha}(k/k-1)]} \tag{13}$$

and

$$S_{k/k-1} = H_{k/k-1} P_{k/k-1} H_{k/k-1}^{\mathrm{T}} + R, \tag{14}$$

where $H_{k/k-1}$ indicates the measurement matrix, computed as the Jacobian of the channel function evaluated at the predicted state, and $P_{k/k-1}$ is the one-step prediction covariance.

When the normalized square innovation

$$\varepsilon(k/k-1) S_{k/k-1}^{-1} \varepsilon(k/k-1) \tag{15}$$

exceeds a threshold (which can be selected either on the basis of a chi-square distribution (Bar-Shalom and Fortmann, 1988) or heuristically), the measurement at time k is not considered as having originated from the tracked reflecting surface (Maksarov and Durrant-White, 1995). In this case the measurement can either be an outlier, or correspond to a new reflecting surface, whose slope has to be evaluated. Where the measurement is an outlier, it is rejected, and the filter performs a prediction step.

To make a decision about the nature of an unpredicted measurement, a bank of n EKFs corresponding to different sea-bed slopes and to a measurement outlier is triggered and run for m steps (decision interval). Then, an Arbiter determines the new bottom slope, evaluating a cost function of each filter residual:

$$\text{filter}_{k/k} = \arg\min_i \sum_{j=0}^{m} \varepsilon_i^2(k-j/k-j-1), \tag{16}$$

where

$$i \in [0\,..\,n] \cap V$$

with

$$V = \{i : \varepsilon_i(j/j-1) S_i^{-1}(j/j-1) \varepsilon_i, (j/j-1) < \delta \quad \forall j \in [k-m, k]\}. \tag{17}$$

V is the set of valid hypotheses after m measurements, i.e. of the hypotheses that satisfy a normalized square innovation test at each step of the decision interval.

Since no "a priori" information is available on the bottom profile, it is not guaranteed that any hypothesized slope will correspond to the real one. A reasonable criterion to tackle this problem is to fix a step $\Delta\alpha$ in the slope variation, and run $n = 2p + 1$ filters with initialized slopes corresponding to

$$\hat{\alpha} - p\Delta\alpha, \ldots, \hat{\alpha} - \Delta\alpha, \hat{\alpha}, \hat{\alpha} + \Delta\alpha, \ldots \hat{\alpha} + p\Delta\alpha \tag{18}$$

(where $\hat{\alpha}$ is the current estimated slope and p a positive integer) and the uncertainty in the slope estimation is of the order of $\Delta\alpha$. The ith hypothesis filter is initialized with

$$\hat{d}_i = \hat{d}\cos(\hat{\alpha}_i)/\cos(\hat{\alpha}). \tag{19}$$

The resulting active multi-hypothesis EKF bottom-estimator scheme is shown in Fig. 3.

5. Application: Romeo bottom follower

The active sonar-based bottom-following system described in the previous sections has been tested on Romeo, an open-frame tethered UUV, designed and developed by the Robotics Department of C.N.R.-I.A.N. for shallow water (up to 500 m depth) marine science applications, and for research in the field of intelligent vehicles. In particular, Romeo has been designed to satisfy marine scientists' requirements of carrying different kinds of payloads, acquiring real-time high-quality video images, and maneuvering with high precision in the proximity of the seabed and man-made underwater structures (Nokin, 1994). To guarantee high precision and agility in maneuvering, great attention has been devoted to propulsion, seeking to ensure maximum controllability and precision on the horizontal plane, while keeping pitch and roll to a minimum. Complete motion controllability is enabled by four horizontal and four vertical thrusters. In addition, environment-based guidance and motion-estimation systems enable the vehicle to perform automatically a number of basic motion tasks in scientific missions.

Fig. 4 shows the vehicle in bottom-following configuration for robotics research. The vehicle weighs about 380 kg in air, and measures $130 \times 90 \times 96$ cm (lwh). The main elements constituting the vehicle are: steel frame, thrusters, buoyancy system, one main cylinder for the electronics, two cylinders for the batteries, one cylinder for the battery chargers, one cylinder for the additional equipment, one cylinder for heading/attitude and inertial sensors (at this time a Watson heading reference unit; Everett, 1995), one package of permanent sensors as CTD (conductivity, temperature, depth), two echosounders, video camera and still camera.

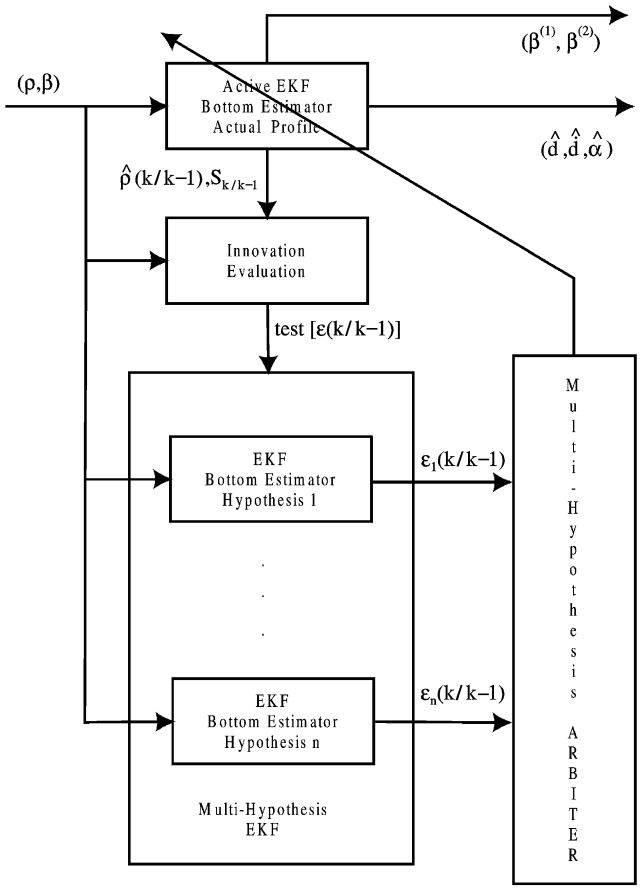

Fig. 3. Active multi-hypothesis extended Kalman filter for bottom estimation.

In high-precision bottom-following applications, the distance of the vehicle from the seabed is measured by a high-frequency (1.25 MHz) pencil-beam profiling sonar Tritech ST-1000. This device is mounted below the vehicle, to track the bottom profile along its longitudinal axis. The profiler sonar head can rotate at increments of 1.8 or 3.6° according to suitable commands received via a RS-232 serial link. Detailed information about the sonar device can be found in Moran (1994) and Cristi et al. (1996).

The software structure is based on the inter-task communication facilities supplied by commercial real-time operating systems. In particular, each task is provided with a set of queues, in which data to be sent to, or received from, other tasks can be stored or retrieved (Bono et al., 1997). As shown in Fig. 5, five synchronous tasks at 10 Hz implement the basic guidance, navigation, motion-estimation, autopilot and sonar-control modules. These tasks exchange commands and replies via message queues, and data by a semaphored shared memory. In particular, the guidance task can activate the motion-estimation procedures required by the maneuver it is executing. Physical devices are piloted by the autopilot and sonar-control tasks. Since the Tritech ST-1000 profiler sonar is asynchronous, it is managed by a dedicated task ("tSt1000" driver), which receives commands from the sonar controller, sends them to the physical device, receives range data and puts them in a dedicated queue. All the sensor data are synchronized by the "input data synchronization task". This task, which is scheduled at 10 Hz, reads data from synchronous A/D and serial devices, as the CTD and heading reference unit, and from asynchronous devices such as the Tritech ST-1000. Raw sensor data are recorded in a shared memory, and made available to the navigation and motion-estimation tasks for filtering. The shared memory also contains controller and filter parameters and reference values.

6. Experimental tests

At sea deployment, the operation and recovery of an underwater vehicle are time consuming and demand

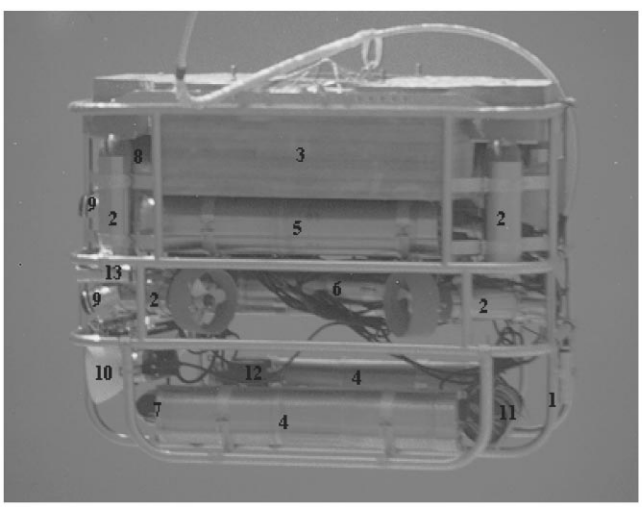

Fig. 4. Romeo in bottom-following pool tests configuration.

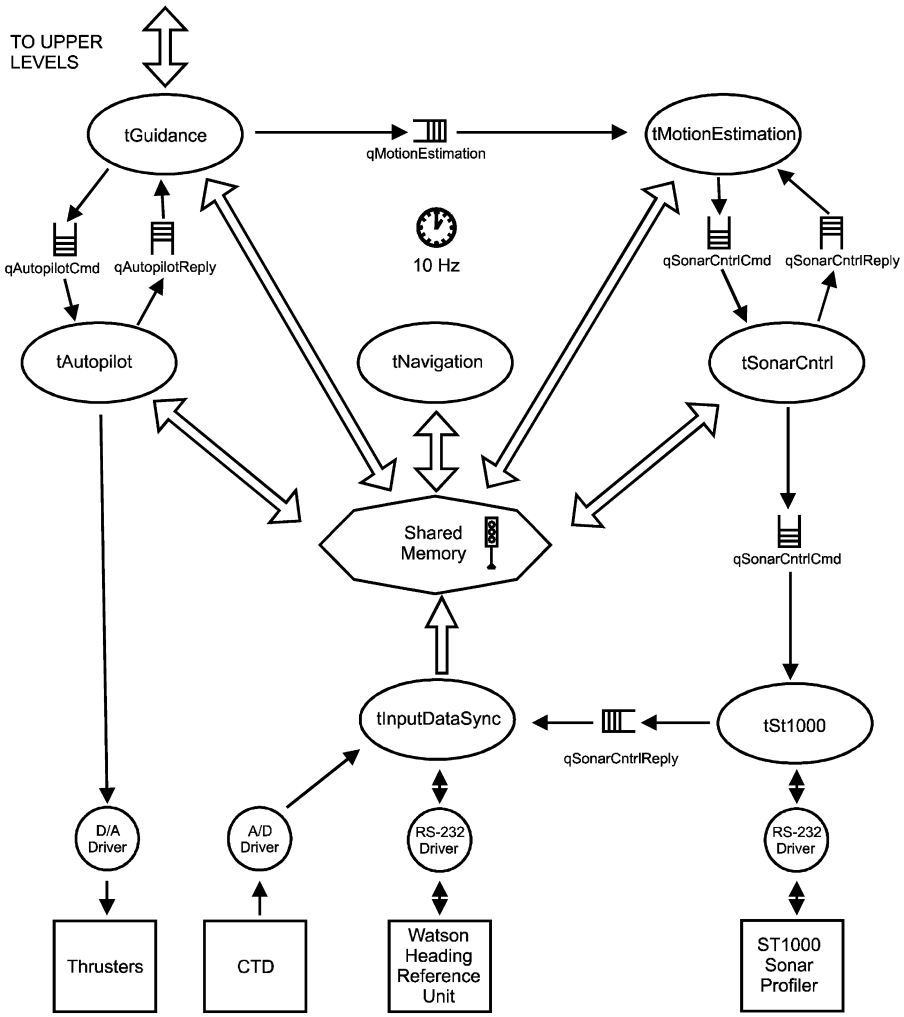

Fig. 5. Romeo's software design.

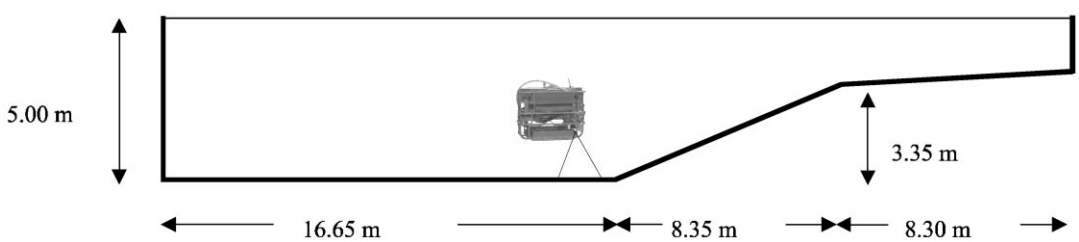

Fig. 6. Genoa pool's bottom profile.

a highly skilled team. In addition, it is quite difficult to perform repeatable tests in the open sea, due to unpredictable and time-varying sea conditions (Bono et al., 1997). For these reasons, some tests can be carried out in enclosed areas such as harbors or pools, where the structure of the operational environment is known, and the vehicle performance can be monitored and evaluated in a set of repetitive tests in quite similar conditions.

On the basis of these considerations, experimental tests have been carried out in a high-diving pool, made available by the Genoa City Council. The pool measures 33.3×23 m, and its bottom profile presents a slope of about 22°. Its maximum depth is about 5 m (see Fig. 6).

The goal of the tests was to evaluate the possibility of maintaining the vehicle at very short range from the bottom (less than 1 m), to allow the acquisition of high-quality video images. Therefore, Romeo was equipped with a Tritech ST-1000 profiler sonar, set for the maximum range of 5 m. The sonar head swept the pool bottom below the vehicle at 1.8° increments, with a sampling frequency of 5 Hz, according to the active sensing techniques discussed in Section 4.

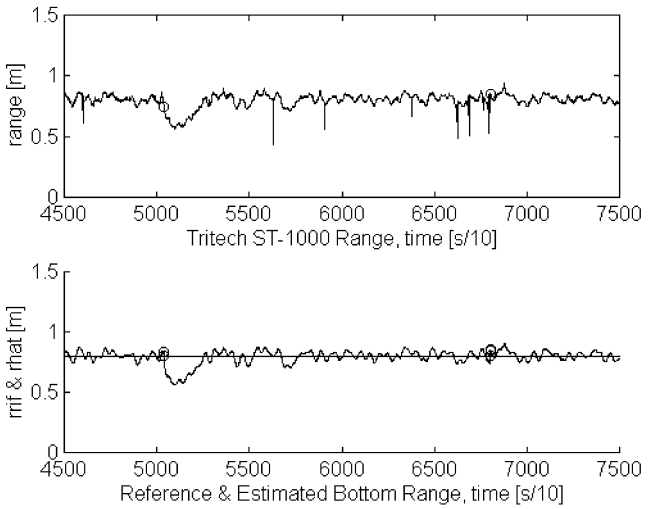

Fig. 7. Tritech ST-1000 range measurements; reference and estimated bottom range (Romeo is moving upwards).

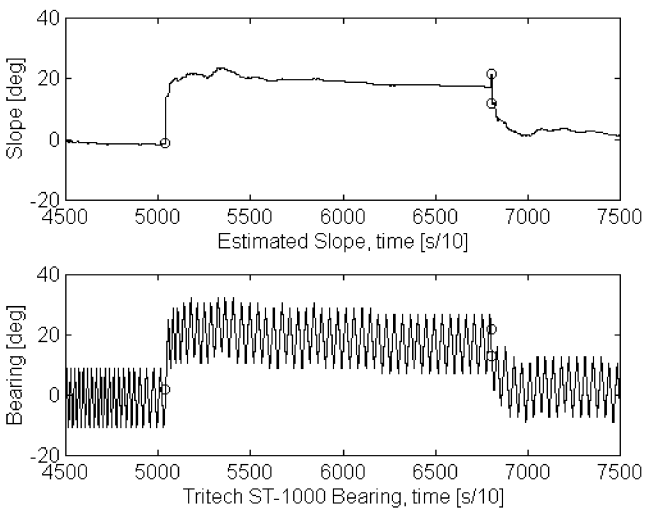

Fig. 8. Estimated bottom slope and Tritech ST-1000 bearing (Romeo is moving upwards).

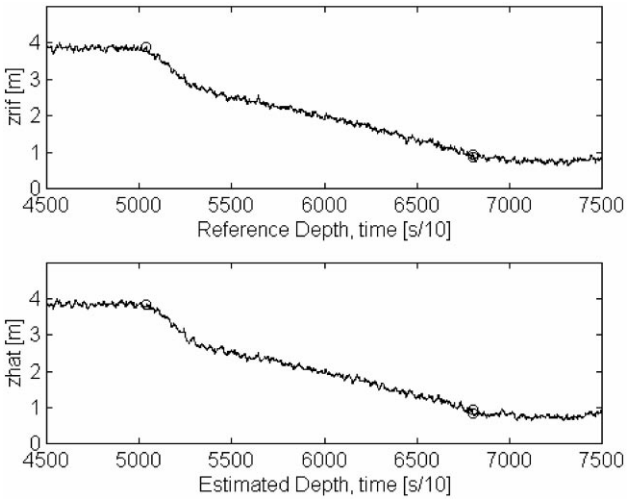

Fig. 9. Reference and estimated depth (Romeo is moving upwards).

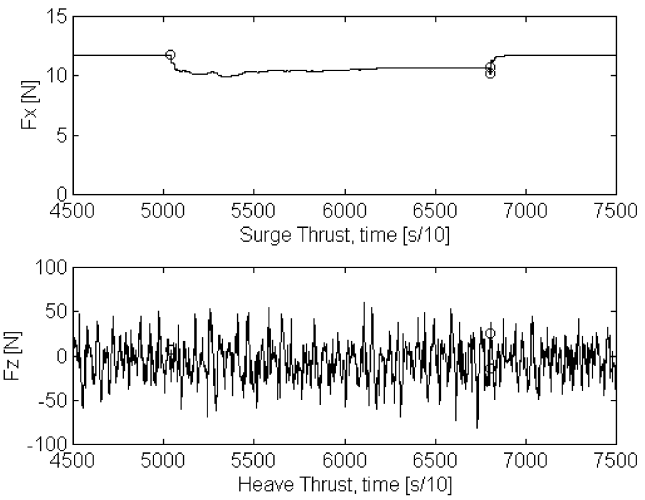

Fig. 10. Longitudinal and vertical thrust (Romeo is moving upwards).

The vehicle moved straight ahead up and down the bottom profile in the direction of maximum slope. Autodepth and autoheading were performed by decoupled PID controllers with a reset function on the integrator. Heading and heading rate measurements were supplied by a Watson heading reference unit. Data supplied by a very shallow water depth-meter (10 m max.) enabled the vehicle depth to be estimated by means of a linear Kalman filter. Surge was controlled in an open loop by fixing a steady-state value of the thrust in the longitudinal direction according to an approximate square relationship with the corresponding vehicle surge.

The covariances of the system and measurement noises are, respectively, $\mathrm{cov}(w_{\hat{d}}) = \mathrm{sqr}(0.01)$, $\mathrm{cov}(w_{\alpha}) = \mathrm{sqr}(0.01\pi/180)$ and $R = \mathrm{cov}(v) = \mathrm{sqr}(0.05)$, while the estimated covariance of each extended Kalman filter is initialized as $P_{\mathrm{init}} = \mathrm{diag}([\mathrm{cov}(\hat{d})\ \mathrm{cov}(\hat{\dot{d}})\ \mathrm{cov}(\hat{\alpha})] = \mathrm{diag}([\mathrm{sqr}(0.5)\ \mathrm{sqr}(0.3)\ \mathrm{sqr}(\Delta\alpha\pi/180)])$, where the range is measured in meters, the linear speed in m/s and the angles in radians. When a possible change in the bottom profile is detected, 7 EKFs are considered, with hypothesized slopes at intervals of $\Delta\alpha = 10^{\circ}$ (see Eq. (18)).

Some test results are presented below.

In the first case, the vehicle followed the ascending profile of the pool at a nominal cruise speed equal to 10 cm/s and a reference distance from the bottom of 80 cm.

Tritech ST-1000 range measurements are plotted in the upper picture of Fig. 7. At short ranges, less than 1 m, the measurement noise is low: the standard deviation is less than 5 cm, considering also the uncertainty related to the vehicle attitude. As shown in the picture, some isolated measurement outliers (spikes) are present and easily detectable. The lower picture of Fig. 7 shows the reference distance from the bottom, together with the

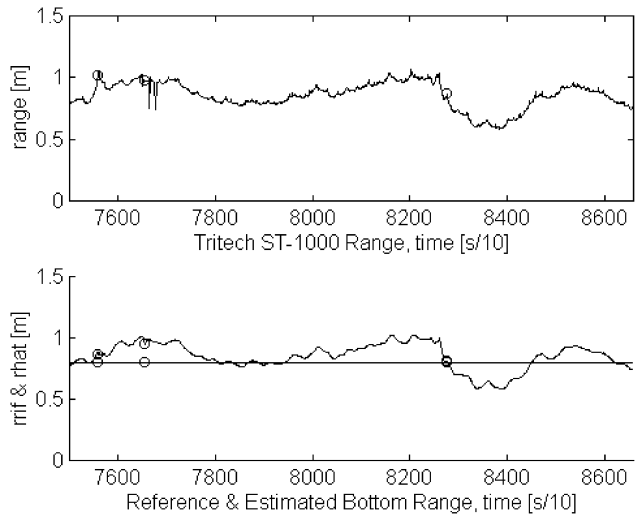

Fig. 11. Tritech ST-1000 range measurements; reference and estimated bottom range (Romeo is moving downwards).

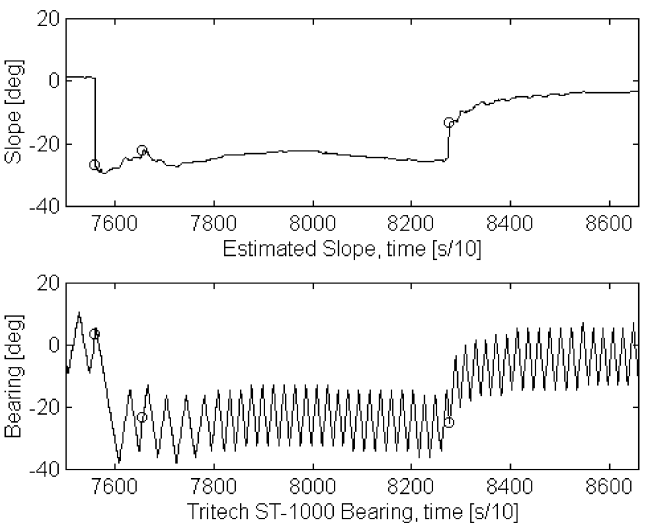

Fig. 12. Estimated bottom slope and Tritech ST-1000 bearing (Romeo is moving downwards).

estimated bottom range, while the estimated bottom slope is plotted in the upper picture of Fig. 8. In each figure, the moments when the bottom profile angle is changed are indicated by circles. As expected, the vehicle distance from the bottom presents a discontinuity when the change in the bottom profile is detected. However, the requested distance from the seabed is quickly tracked again, and, except during this transition phase, the estimated bottom distance error is always lower than 10 cm. In these operational conditions, the TV cameras mounted on the vehicle could acquire very stable and well-defined images of the pool floor. As shown in the lower picture of Fig. 8, active sensing keeps the sonar sweep centered on the direction perpendicular to the estimated slope.

On the basis of the estimated distance from the bottom, the reference heave and depth are computed according to the formulae (7) and (9), respectively. Fig. 9 shows the reference and estimated depth.

The control actions, which are the vertical and horizontal thrusts applied to the vehicle, are plotted in Fig. 10. In particular, the upper picture, where the thrust applied to the vehicle in the longitudinal direction is plotted, shows how the vehicle surge decreases when the bottom slope decreases to maintain the motion parallel to the seabed profile, as stated in Eq. (7). The lower picture shows the vertical thrust applied to the vehicle.

The results of a test performed with Romeo moving along the descent profile of the pool are given below.

Also in this case, the range measurements are characterized by noise with standard deviation of about 5 cm, and by the presence of some outliers as shown in the upper picture of Fig. 11. Although the performance of the active bottom estimator is good, the bottom slope changes are immediately detected, and the slope estimate is stable and precise (see Fig. 12), the performance in bottom range control is worse than in the previous case (see Fig. 11, lower picture). Anyway, the vehicle is always maintained at a range from the bottom, of less than 1.1 m. In this way, the TV camera used to pilot the vehicle, which usually looks ahead and downwards, can collect video images of the pool floor, even when the vehicle moves down. This fact facilitates the intervention of the human operator, enabling him/her to maintain continuous visual feedback from the seabed with a fixed camera. A set of bottom-following tests have been performed keeping Romeo within different range from the pool bottom. Results are quite similar to those of the cases previously discussed.

Since the depth signal was rather noisy, and (in order to be able to track the system dynamics even in the presence of high vertical thruster forces), the linear Kalman filter for depth estimation had been tuned with a fairly high covariance of the system noise, the estimated depth $\hat{z}$ can be sufficiently noisy to make $\text{sign}(z^*_{t+\Delta t} - z^*_t) \neq \text{sign}(\dot{z}^*)$ with $t \in [t_0, t_1]$ and $\text{sign}(\dot{z}^*) = \text{const}$ for $t \in [t_0, t_1]$, where z^* is computed as shown in Eq. (9).

This fact can induce a reduction in performance, as in the second experiment discussed above.

On this basis, current research at CNR-IAN is being focused on the identification of the hydrodynamic derivatives of the vehicle in order to implement more precise dynamic motion estimators, and on the design, implementation and testing of a UUV autopilot constituted of basic nonlinear velocity controllers. Such an autopilot could then be interfaced with a task-function-based guidance system, able to generate the desired linear and angular velocities on the basis of the specified tasks, e.g. "bottom following at fixed distance", where the desired surge and heave are computed according to Eq. (7).

7. Conclusions

This paper addresses the problem of accurate bottom-following for UUVs moving at low speeds in the proximity of the seabed. Its accomplishment is required by many applications in marine science and off-shore operations. The proposed solution is based on the integration of active multi-hypothesis EKF motion and environment estimation techniques, Lyapunov-based guidance systems and a conventional UUV autopilot. The resulting bottom-following architecture can operate on a large class of advanced UUVs, and has been operationally tested on Romeo, a UUV prototype developed by C.N.R.-I.A.N.

Pool test results have revealed the feasibility of the method, which can be easily implemented in a real-time control architecture for UUVs. In particular, the method enables the system to perform the bottom-following task with the high degree of precision required by operational applications as (semi-)automatic video monitoring of benthic areas. The vehicle is able to maintain a constant range from the bottom, of less than 1 m.

Current research is focused on enhancing system performance by implementing model-based dynamic motion estimators and a velocity control-based autopilot, which more naturally matches with a task-based guidance and control system.

Acknowledgements

The authors wish to thank all the staff at the Genoa City Council's Sports Authority for granting access to the municipal pool for testing.

This work was partially funded by PNRA (Programma Nazionale di Ricerche in Antartide), Task 4a – Robotica e Telescienza in Ambiente Estremo.

References

Bar-Shalom, Y., & Fortmann, T.E. (1988). *Tracking and data association*. San Diego: Academic Press.

Bennett, A.A., Leonard, J.J., & Bellingham, J.G. (1995). Bottom following for survey-class autonomous underwater vehicles. *Proc. 9th Int. Symp. on Unmanned Untethered Submersible Technology*, Durham, USA (pp. 327–336).

Bono, R., Bruzzone, G., Caccia, M., Veruggio, G., & Virgili, P. (1997). A real-time architecture for development and control of unmanned underwater vehicles. *Proc. 4th Workshop on Algorithms and Architectures for Real-Time Control*, Vilamoura, Portugal.

Caccia, M., Veruggio, G., Casalino, G., Alloisio, S., Grosso, C., & Cristi, R. (1997). Sonar-based bottom estimation in UUVs adopting a multi-hypothesis extended Kalman filter. *Proc. 8th Int. Conf. on Robotics*, Monterey, USA (pp. 745–750).

Caccia, M., Casalino, G., Cristi, R., & Veruggio, R. (1998). Acoustic motion estimation and control for an unmanned underwater vehicle in a structured environment, Oxford: Pergamon Press. *Control Engineering Practice*, *6*(5), 661–670.

Cristi, R., Caccia, M., & Veruggio, G. (1996). Motion estimation and modeling of the environment for underwater vehicles. *Proc. 6th IARP in Underwater Robotics*, Toulon, France.

Everett, H.R. (1995). *Sensors for mobile robots – theory and application*. Wellesley, USA: A. K. Peters Ltd.

Fossen, T.I. (1994). *Guidance and control of ocean vehicles*. New York, UK: Wiley.

Maksarov, D., & Durrant-White, H. (1995). Mobile vehicle navigation in unknown environments: A multiple hypothesis approach. *IEE Proc.-Control Theory Appl.*, *142*(4), 385–400.

Moran, B.A. (1994). *Underwater shape reconstruction in two dimensions*. Ph.D. thesis, MIT, Cambridge, MA.

Nokin, M. (1994). ROV 6000–objectives and description. *Proc. of Oceans'94*, Brest, France (Vol. 2, pp. 505–510).

Samson, C., Le Borgne, M., & Espiau, B. (1991). *Robot control: the task function approach*. Oxford Science Publications, Oxford Engineering Science Series, (Vol. 22). Oxford, Great Britain: Clarendon Press.

Santos, A.S., Simon, D., & Rigaud, V. (1995a). Sensor-based control of a class of underactuated autonomous underwater vehicles. *Proc. 3rd IFAC Workshop on Control Applications in Marine Systems*, Trondheim, Norway (pp. 107–114).

Santos, A.S., Rives, P., Espiau, B., & Simon, D. (1995b). Dealing in real-time with a priori unknown environment on autonomous underwater vehicles (AUVs). *Proc. Robotics Automat.* Nagoya, Japan (Vol. 2, pp. 1579–1584).

Sayers, C., Yoerger, D.R., & Paul, R.P. (1996). A manipulator work package for teleoperation from unmanned untethered vehicles–current feasibility and future applications. *Proc. 6th Int. Adv. Robotic Program*, Toulon, France.

Sheridan, T.B. (1989). Telerobotics. *Automatica*, *25*(4), 487–507.

Swayn, M.J., & Stricker, M.A. (1993). Promising directions in active vision. *Int. J. Comput. Vision*, *11*(2), 109–126.

Veruggio, G., Caccia, M., & Bono, R. (1996). ROMEO: A test-bed vehicle for the Virtual Lab. *6th IARP in Underwater Robotics*, Toulon, France.